

High order numerical methods for nonlinear wave equations

Yan Xu

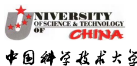
yxu@ustc.edu.cn

<http://staff.ustc.edu.cn/~yxu/>

School of Mathematical Sciences
University of Science and Technology of China

Joint with Chi-Wang Shu
shu@dam.brown.edu
Division of Applied Mathematics
Brown University

Supported by **NSFC**

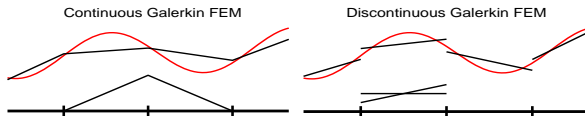


Outline

- 1 Introduction to local discontinuous Galerkin (LDG) methods
- 2 The LDG method for the Camassa-Holm equation
- 3 LDG method for the Degasperis-Procesi equation
- 4 Numerical results
 - Numerical results for the CH equation
 - Numerical results for Degasperis-Procesi equation
- 5 Conclusion and future work

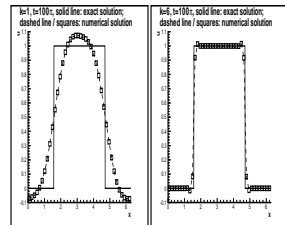
Discontinuous Galerkin Methods

- Finite element method for approximating PDE.
- Piecewise polynomial completely discontinuous.

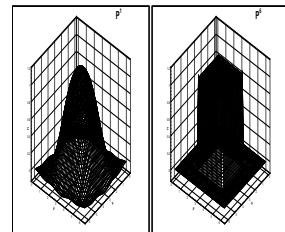


- Local variational formulation (element-by-element).
- First introduced in 1973 by Reed and Hill.
- Hyperbolic conservation law by Cockburn and Shu.
- According the search in Mathscinet, papers with key words “**Discontinuous Galerkin**”
 - Before 2000, 203 papers;
 - 2001-2014, **2357** papers.

1D Transport



2D Transport



Advantages of DG methods:

- ✓ Wide Range of PDE's
- ✓ Easy handling complicated geometry and boundary conditions
- ✓ Allowing the hanging nodes
- ✓ Compact and then parallel efficiency.
- ✓ Easy $h - p$ adaptivity;
- ✓ Flexible choice of approximation spaces

Disadvantages of DG methods:

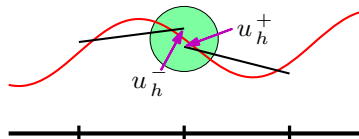
- × more of degrees of freedom
- × Systems of equations difficult to solve
- × Techniques under development

Numerical fluxes

Double-valued, need to pick/define one

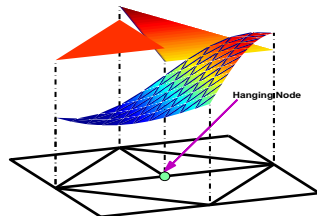
$$\widehat{f}(u_h) = \widehat{f}(u_h^-, u_h^+)$$

$$\widehat{u}_h = \widehat{u}(u_h^-, u_h^+)$$



Hanging node

Nonconforming Mesh and Variable Degree



DG scheme for hyperbolic conservation laws

$$u_t + f(u)_x = 0.$$

Multiplying with a test function

$$v \in V_h = \{v : v|_{I_j} \in P^k(I_j), j = 1, \dots, N\}$$

and integrating by parts over a cell $I_j = [x_{j-1/2}, x_{j+1/2}]$, DG scheme:
Find $u \in V_h$ such that, for all $v \in V_h$ and $j = 1, \dots, N$

$$\int_{I_j} u_t v dx - \int_{I_j} f(u) v_x dx + \hat{f}_{j+\frac{1}{2}} v_{j+\frac{1}{2}}^- - \hat{f}_{j-\frac{1}{2}} v_{j-\frac{1}{2}}^+ = 0.$$

\hat{f} is the single value monotone numerical flux:

$$\hat{f}_{j+\frac{1}{2}} = \hat{f}(u_{j+\frac{1}{2}}^-, u_{j+\frac{1}{2}}^+)$$

where $\hat{f}(u, u) = f(u)$ (consistency); $\hat{f}(\uparrow, \downarrow)$ (monotonicity) and \hat{f} is Lipschitz continuous with respect to both arguments.

Introduction to local discontinuous Galerkin (LDG) methods:

Generalization of the DG method to PDEs containing higher spatial derivatives. For example, the heat equation

$$u_t - u_{xx} = 0$$

with proper boundary and initial conditions.

A straightforward generalization is replacing $f(u) = -u_x$ in the DG scheme for the conservation law ($u_t + f(u)_x = 0$): find $u \in V_h$ such that, for all test functions $v \in V_h$,

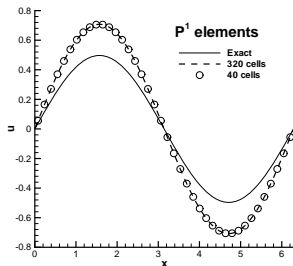
$$\int_{I_j} u_t v dx + \int_{I_j} u_x v_x dx - \widehat{u}_{x_{j+\frac{1}{2}}} v_{j+\frac{1}{2}} + \widehat{u}_{x_{j-\frac{1}{2}}} v_{j-\frac{1}{2}} = 0.$$

Considering that diffusion is isotropic, a nature choice of the flux could be the central flux

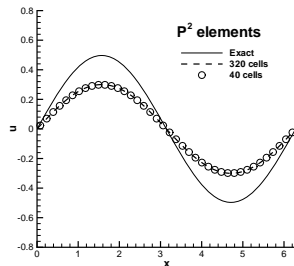
$$\widehat{u}_{x_{j+\frac{1}{2}}} = \frac{1}{2} \left((u_x)_{j+\frac{1}{2}}^- + (u_x)_{j+\frac{1}{2}}^+ \right)$$

However, it has been proven in Zhang and Shu, M³AS 03 that the scheme is

- Consistent with the heat equation
- (very weakly) unstable



(a) u , $t = 6$.



(b) v , $t = 6$.

The LDG method for the heat equation (Bassi and Rebay, JCP 97; Cockburn and Shu, SINUM 98):

- Rewrite the heat equation as

$$u_t - q_x = 0, \quad q - u_x = 0.$$

- Find $u, q \in V_h$ such that, for all $v, w \in V_h$,

$$\int_{I_j} u_t v dx + \int_{I_j} q v_x - \hat{q}_{j+\frac{1}{2}} v_{j+\frac{1}{2}}^- + \hat{q}_{j-\frac{1}{2}} v_{j-\frac{1}{2}}^+ = 0,$$

$$\int_{I_j} q p dx + \int_{I_j} u p_x - \hat{u}_{j+\frac{1}{2}} p_{j+\frac{1}{2}}^- + \hat{u}_{j-\frac{1}{2}} p_{j-\frac{1}{2}}^+ = 0.$$

q can be **locally** solved and eliminated, hence local DG.

The numerical flux is the following alternated flux

$$\hat{u}_{j+\frac{1}{2}} = u_{j+\frac{1}{2}}^-, \quad \hat{q}_{j+\frac{1}{2}} = q_{j+\frac{1}{2}}^+,$$

or

$$\hat{u}_{j+\frac{1}{2}} = u_{j+\frac{1}{2}}^+, \quad \hat{q}_{j+\frac{1}{2}} = q_{j+\frac{1}{2}}^-.$$

Then we have

- L^2 stability
- Optimal convergence of $\mathcal{O}(h^{k+1})$ in L^2 for P^k elements.

Table: L^2 and L^∞ errors and orders of accuracy for the LDG method with alternated fluxes applied to the heat equation with an initial condition $u(x, 0) = \sin(x)$, $t = 1$. Third order Runge-Kutta in time with a small Δt so that time error can be ignored.

Δx	$k = 1$				$k = 2$			
	L^2 error	order	L^∞ error	order	L^2 error	order	L^∞ error	order
$2\pi/20, u$	1.58E-03	—	6.01E-03	—	3.98E-05	—	1.89E-04	—
$2\pi/20, q$	1.58E-03	—	6.01E-03	—	3.98E-05	—	1.88E-04	—
$2\pi/40, u$	3.93E-04	2.00	1.51E-03	1.99	4.98E-06	3.00	2.37E-05	2.99
$2\pi/40, q$	3.94E-04	2.00	1.51E-03	1.99	4.98E-06	3.00	2.37E-05	2.99
$2\pi/80, u$	9.83E-05	2.00	3.78E-04	2.00	6.22E-07	3.00	2.97E-06	3.00
$2\pi/80, q$	9.83E-05	2.00	3.78E-04	2.00	6.22E-07	3.00	2.97E-06	3.00
$2\pi/160, u$	2.46E-05	2.00	9.45E-05	2.00	7.78E-08	3.00	3.71E-07	3.00
$2\pi/160, q$	2.46E-05	2.00	9.45E-05	2.00	7.78E-08	3.00	3.71E-07	3.00

Main idea of LDG method for high order derivative equations

- Rewrite the high order derivative term into the **proper** first order equations.
- Use the DG method for the first order equations.
- The key point of the method is to design the numerical fluxes to ensure the stability.
 - Odd derivatives equation: upwinding principle.
 - Even derivatives equation: alternating fluxes.

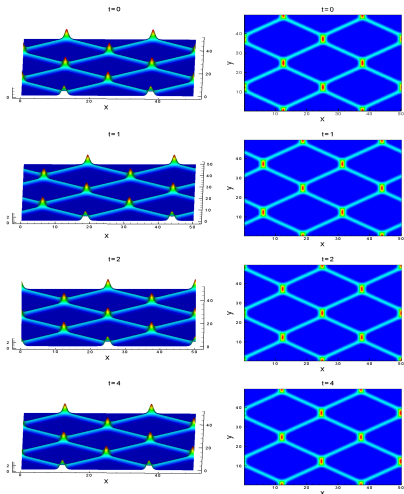
Review paper

- Y. Xu and C.-W. Shu, Local discontinuous Galerkin methods for high-order time-dependent partial differential equations, Communications in Computational Physics, 7 (2010), pp. 1-46.

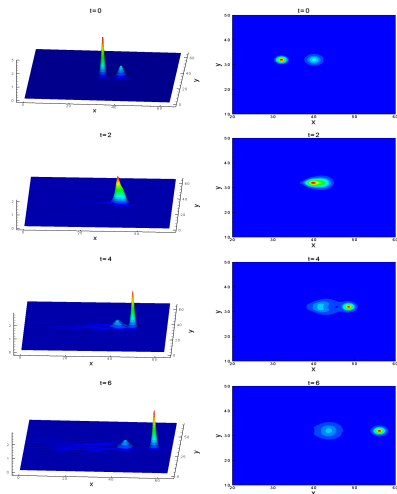
LDG methods for nonlinear dispersive equations

- KdV equation (Yan and Shu SINUM 2002, Xu-Shu CMAME 2007).
- KdV-Burgers equation, Kawahara equation (Xu-Shu, JCM 2004).
- Fully nonlinear $K(m, n)$ and $K(n, n, n)$ equations(Levy-Shu-Yan JCP 2004, Xu-Shu JCM 2004).
- Kadomtsev-Petviashvili equation (Xu-Shu, Physica D 2005).
- Zakharov-Kuznetsov equation (Xu-Shu Physica D 2005, Xu-Shu CMAME 2007).
- Ito-type coupled KdV equations (Xu-Shu CMAME 2006).

Kadomtsev-Petviashvili equation (Physica D, 2005)



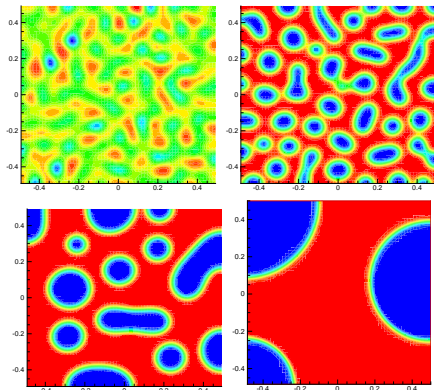
Zakharov-Kuznetsov equation (Physica D, 2005)



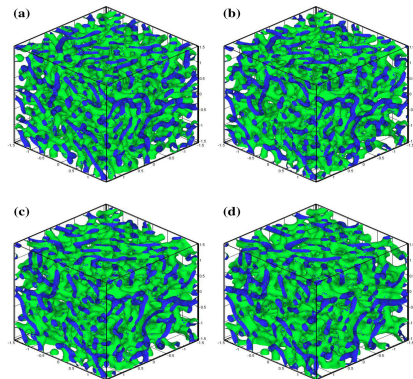
LDG methods for phase field models

- Cahn-Hilliard equation ([Xia-Xu-Shu JCP 2007](#), [Guo-Xu JSC 2014](#))
- Allen-Cahn/Cahn-Hilliard system ([Xia-Xu-Shu, CACP 2009](#))
- Functionalized Cahn-Hilliard equation ([Guo-Xu-Xu, JSC 2015](#))
- No-slop-selection thin film model ([Xia, JCP 2015](#))
- Cahn-Hilliard-Hele-Shaw system ([Guo-Xia-Xu, JCP 2014](#))
- Cahn-Hilliard-Brinkman system ([Guo-Xu, JCP 2015](#))
- Phase field crystal equation ([Guo-Xu, submitted](#))

2D Cahn-Hilliard equation (JSC, 2014)



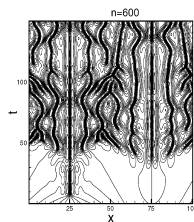
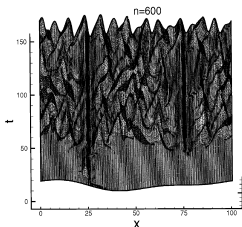
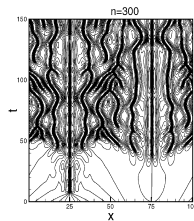
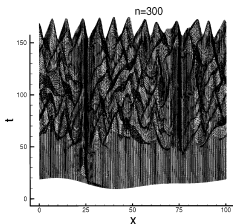
3D Functionalized Cahn-Hilliard (JSC, 2015)



LDG methods for nonlinear diffusion equations

- Bi-harmonic equations (Yan-Shu JSC 2002, Dong-Shu SINUM 2009).
- Kuramoto-Sivashinsky equation (Xu-Shu, CMAME 2006).
- Surface diffusion of graphs and Willmore flow of graphs (Xu-Shu JSC 2009, Ji-Xu submitted 2009).
- Porous medium equation (Zhang-Wu JSC 2009).

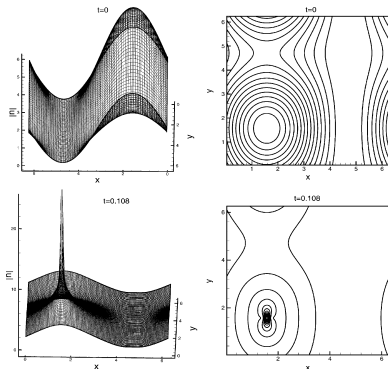
Kuramoto-Sivashinsky (CMAME 2006)



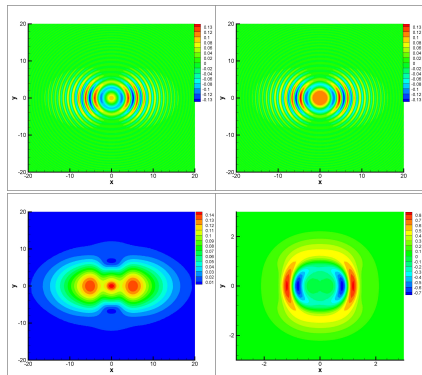
LDG methods for Schrödinger equation

- Nonlinear Schrödinger equations (Xu-Shu JCP 2005, Lu-Cai-Zhang IJAM 2005)
- Zakharov system (Xia-Xu-Shu JCP 2010)
- Stationary Schrödinger equations (Wang-Shu JSC 2009, Guo-Xu CICIP 2014)
- Nonlinear Schrödinger-KdV System (Xia-Xu-Shu CICIP 2014)
- Nonlinear Schrödinger equation with wave operator (Guo-Xu JSC 2014)

2D Schrödinger equation (JCP, 2005)



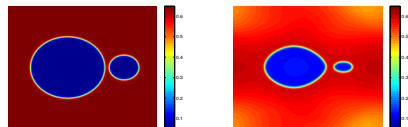
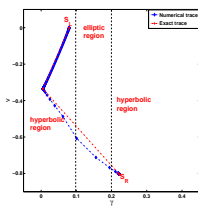
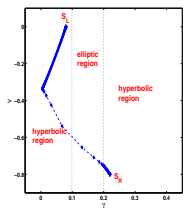
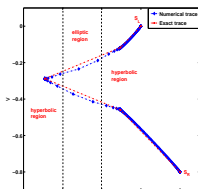
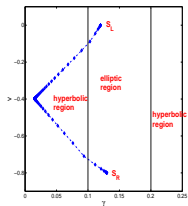
2D Zakharov system (JCP, 2010)



LDG methods for phase transition problems

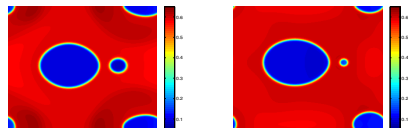
1D phase transition in solid (JSC 2014)

Navier-Stokes-Korteweg (JCP, 2015)



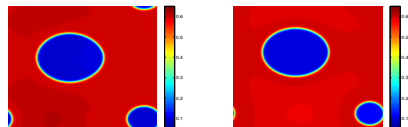
(a) $t=0$

(b) $t=1$



(c) $t=2$

(d) $t=3$



LDG methods for other equations

- Degasperis-Procesi (DP) equation (Xu-Shu, CICP 2011).

$$u_t - u_{xxt} + 4uu_x = 3u_x u_{xx} + uu_{xxx}$$

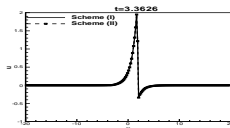
- Camassa-Holm (CH) equation (Xu-Shu, SINUM 2008).

$$u_t - u_{xxt} + 3uu_x = 2u_x u_{xx} + uu_{xxx}.$$

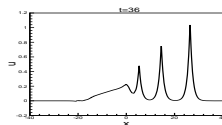
- Hunter-Saxton (HS) equation (Xu-Shu, SIJSC 2008 and JCM 2010).

$$u_{xxt} + 2u_x u_{xx} + uu_{xxx} = 0$$

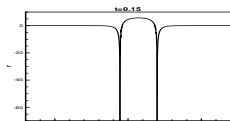
Degasperis-Procesi (CICP)



Camassa-Holm (SINUM)



Hunter-Saxton (SIJSC)



Family of third order dispersive PDE conservation laws

$$u_t + c_0 u_x + \kappa u_{xxx} - \epsilon^2 u_{txx} = (c_1 u^2 + c_2 u_x^2 + c_3 uu_{xx})_x,$$

where κ , ϵ , c_0 , c_1 , c_2 , and c_3 are real constants.

Integrability

There are only three equations that satisfy the asymptotic integrability condition within this family

- KdV equation ($\epsilon = c_2 = c_3 = 0$).
- Camassa-Holm equation ($c_1 = -\frac{3c_3}{2\epsilon^2}$, $c_2 = \frac{c_3}{2}$).
- Degasperis-Procesi ($c_1 = -\frac{2c_3}{2\epsilon^2}$, $c_2 = c_3$).

Camassa-Holm (CH) equation

$$u_t - u_{xxt} + 3uu_x = 2u_x u_{xx} + uu_{xxx}.$$

Degasperis-Procesi (DP) equation

$$u_t - u_{xxt} + 4uu_x = 3u_x u_{xx} + uu_{xxx}$$

Energy

Camassa-Holm (CH) equation

$$H_2(u) = \int_R (u^2 + u_x^2) dx$$

Degasperis-Procesi (DP) equation

$$E_2(u) = \int_R (u - u_{xx})v dx, \quad 4v - \partial_x^2 v = u$$

Solution

Camassa-Holm (CH) equation

- Peaked Solution
- No shock wave solutions with initial data $u_0 \in H^1(\mathbb{R})$

Degasperis-Procesi (DP) equation

- Peaked Solution
- Shock wave solutions

- 1 Introduction to local discontinuous Galerkin (LDG) methods
- 2 The LDG method for the Camassa-Holm equation
- 3 LDG method for the Degasperis-Procesi equation
- 4 Numerical results
 - Numerical results for the CH equation
 - Numerical results for Degasperis-Procesi equation
- 5 Conclusion and future work

Camassa-Holm (CH) equation

$$u_t - u_{xxt} + 2\kappa u_x + 3uu_x = 2u_x u_{xx} + uu_{xxx},$$

where κ is a constant.

- u representing the free surface of water over a flat bed.
- A model for the propagation of the unidirectional gravitational waves in a shallow water approximation.
- It is completely integrable.
- It models wave breaking for a large class of initial data.

Energy

$$H_2(u) = \int_R (u^2 + u_x^2) dx$$

Numerical challenge

- Such nonlinearly dispersive partial differential equations support peakon solutions.
- The lack of smoothness at the peak of the peakon introduces high-frequency dispersive errors into the calculation.
- It is a challenge to design stable and high-order accurate numerical schemes for solving this equation.

Equation

$$u - u_{xx} = q, \quad (1)$$

$$q_t + f(u)_x = \frac{1}{2}(u^2)_{xxx} - \frac{1}{2}((u_x)^2)_x \quad (2)$$

The LDG method

- we rewrite the equation (1) as a first order system:

$$u - r_x = q,$$

$$r - u_x = 0.$$

- q is assumed known and we would want to solve for u . The LDG method is formulated as follows: find $u_h, r_h \in V_h$ such that, for all test functions $\rho, \phi \in V_h$,

$$\int_{I_j} u_h \rho dx + \int_{I_j} r_h \rho_x dx - (\hat{r}_h \rho^-)_{j+\frac{1}{2}} + (\hat{r}_h \rho^+)_{j-\frac{1}{2}} = \int_{I_j} q_h \rho dx,$$

$$\int_{I_j} r_h \phi dx + \int_{I_j} u_h \phi_x dx - (\hat{u}_h \phi^-)_{j+\frac{1}{2}} + (\hat{u}_h \phi^+)_{j-\frac{1}{2}} = 0.$$

- Numerical flux: $\hat{r}_h = r_h^-$, $\hat{u}_h = u_h^+$.

The LDG method (continued)

- For the equation (2), we can also rewrite it into a first order system:

$$\begin{aligned}q_t + f(u)_x - p_x + B(r)_x &= 0, \\ p - (b(r)u)_x &= 0, \\ r - u_x &= 0,\end{aligned}$$

where $B(r) = \frac{1}{2}r^2$ and $b(r) = B'(r) = r$.

The LDG method (continued)

- Now we can define a local discontinuous Galerkin method, resulting in the following scheme: find $q_h, p_h, r_h \in V_h$ such that, for all test functions $\varphi, \psi, \eta \in V_h$,

$$\begin{aligned} & \int_{I_j} (q_h)_t \varphi dx - \int_{I_j} (f(u_h) - p_h + B(r_h)) \varphi_x dx \\ & + ((\widehat{f} - \widehat{p}_h + \widehat{B}(r_h)) \varphi^-)_{j+\frac{1}{2}} - ((\widehat{f} - \widehat{p}_h + \widehat{B}(r_h)) \varphi^+)_{j-\frac{1}{2}} = 0, \\ & \int_{I_j} p_h \psi dx + \int_{I_j} b(r_h) u_h \psi_x dx - (\widehat{b}(r_h) \widetilde{u}_h \psi^-)_{j+\frac{1}{2}} + (\widehat{b}(r_h) \widetilde{u}_h \psi^+)_{j-\frac{1}{2}} = 0, \\ & \int_{I_j} r_h \phi dx + \int_{I_j} u_h \eta_x dx - (\widehat{u}_h \eta^-)_{j+\frac{1}{2}} + (\widehat{u}_h \eta^+)_{j-\frac{1}{2}} = 0. \end{aligned}$$

Numerical flux

- Alternate numerical fluxes

$$\widehat{p}_h = p_h^-, \widehat{u}_h = u_h^+, \widehat{B}(r_h) = B(r_h^-), \widetilde{u}_h = u_h^+.$$

- Central numerical flux

$$\widehat{b}(r_h) = \frac{B(r_h^+) - B(r_h^-)}{r_h^+ - r_h^-}$$

- $\widehat{f}(u_h^-, u_h^+)$

- Central numerical flux:

$$\widehat{f}(u_h^-, u_h^+) = \frac{1}{2}(f(u_h^-) + f(u_h^+)),$$

- Lax-Friedrichs flux

$$\widehat{f}(u_h^-, u_h^+) = \frac{1}{2}(f(u_h^-) + f(u_h^+) - \alpha(u_h^+ - u_h^-)), \quad \alpha = \max |f'(u_h)|$$

Algorithm flowchart

- We obtain \mathbf{q}_h in the following matrix form

$$\mathbf{q}_h = \mathbf{A}\mathbf{u}_h.$$

- we obtain the LDG discretization of the residual $-f(u)_x + \frac{1}{2}(u^2)_{xxx} - \frac{1}{2}((u_x)^2)_x$ in the vector form

$$(\mathbf{q}_h)_t = \mathbf{res}(\mathbf{u}_h).$$

- We then combine the above two equation to obtain

$$\mathbf{A}(\mathbf{u}_h)_t = \mathbf{res}(\mathbf{u}_h).$$

- We use a time discretization method to solve

$$(\mathbf{u}_h)_t = \mathbf{A}^{-1}\mathbf{res}(\mathbf{u}_h).$$

L^2 stability of the LDG method

The solution to the LDG schemes for the Camassa-Holm equation satisfies the L^2 stability

- $\hat{f}(u_h^-, u_h^+)$: central numerical flux

$$\frac{d}{dt} \int_0^L (u_h^2 + r_h^2) dx = 0.$$

- $\hat{f}(u_h^-, u_h^+)$: Lax-Friedrichs flux

$$\frac{d}{dt} \int_0^L (u_h^2 + r_h^2) dx \leq 0.$$

The main error estimate result

Let u be the exact solution of the Camassa-Holm equation, which is sufficiently smooth with bounded derivatives, and assume $f \in C^3$. For regular triangulations of $I = (0, 1)$, if the finite element space V_h is the piecewise polynomials of degree $k \geq 2$, then for small enough h there holds the following error estimates

$$\|u - u_h\|^2 + \|r - r_h\|^2 \leq Ch^{2k}, \quad (3)$$

where the constant C depends on the final time T , k , $\|u\|_{k+1}$, $\|r\|_{k+1}$ and the bounds on the derivatives $|f^{(m)}|$, $m = 1, 2, 3$. Here $\|u\|_{k+1}$ and $\|r\|_{k+1}$ are the maximum over $0 \leq t \leq T$ of the standard Sobolev $k + 1$ norm in space.

Remark

- Although we could not obtain the optimal error estimates $O(h^{k+1})$ for u due to some extra boundary terms arising from high order derivatives, numerical examples verify the optimal order $O(h^{k+1})$ for u .
- For the solution r_h , our numerical results indicate that k -th order accuracy is sharp.

Main difficulty of the proof

- Nonlinear term.
- Lack of control on some of the jump terms at cell boundaries for high order derivatives term.
- Special projection is introduced to handle troublesome jump terms in the error equation.
- It is more challenging to perform L^2 *a priori* error estimates for nonlinear PDEs with high order derivatives than for first order hyperbolic PDEs

- 1 Introduction to local discontinuous Galerkin (LDG) methods
- 2 The LDG method for the Camassa-Holm equation
- 3 LDG method for the Degasperis-Procesi equation
- 4 Numerical results
 - Numerical results for the CH equation
 - Numerical results for Degasperis-Procesi equation
- 5 Conclusion and future work

Degasperis-Procesi equation

$$u_t - u_{txx} + 4f(u)_x = f(u)_{xxx},$$

where $f(u) = \frac{1}{2}u^2$.

- DP equation support peakon solutions and shock solutions.
- The lack of smoothness of the solution introduces more difficulty in the numerical computation.

Energy

Camassa-Holm (CH) equation

$$H_2(u) = \int_R (u^2 + u_x^2) dx$$

Degasperis-Procesi (DP) equation

$$E_2(u) = \int_R (u - u_{xx})v dx, \quad 4v - \partial_x^2 v = u$$

Numerical difficulty

- Conservation laws of the DP equation are much weaker than those of the CH equation
- The conservation laws $E_i(u)$ can not guarantee the boundedness of the slope of a wave in the L^2 -norm.
- There is no way to find conservation laws controlling the H^1 -norm, which plays a very important role in studying the CH equation.

L^2 stability

- Auxiliary variable v which satisfies the following equation

$$4v - v_{xx} = u.$$

- Another form of the energy $E_2(u)$

$$\frac{d}{dt} \int_{\Omega} \left(2v^2 + \frac{5}{2}(v_x)^2 + \frac{1}{2}(v_{xx})^2 \right) dx = 0.$$

- L^2 stability of u , i.e.

$$\|u\|_{L^2(R)} \leq 2\sqrt{2} \|u_0\|_{L^2(R)}.$$

LDG scheme (I) based on dispersive form

We write the DP equation in the following form

$$u - u_{xx} = q, \quad (4)$$

$$q_t + 4f(u)_x = f(u)_{xxx}. \quad (5)$$

The LDG method (I) continued

- we rewrite the equation (4) as a first order system:

$$q - r_x = 0,$$

$$r - u_x = 0.$$

- q is assumed known and we would want to solve for u . The LDG method is formulated as follows: find $u_h, r_h \in V_h$ such that, for all test functions $\rho, \phi \in V_h$,

$$\int_{I_j} q_h \rho dx + \int_{I_j} r_h \rho_x dx - (\hat{r}_h \rho^-)_{j+\frac{1}{2}} + (\hat{r}_h \rho^+)_{j-\frac{1}{2}} = 0,$$

$$\int_{I_j} r_h \phi dx + \int_{I_j} u_h \phi_x dx - (\hat{u}_h \phi^-)_{j+\frac{1}{2}} + (\hat{u}_h \phi^+)_{j-\frac{1}{2}} = 0.$$

- Numerical flux: $\hat{r}_h = r_h^-$, $\hat{u}_h = u_h^+$.

The LDG method (I) continued

For the equation (5), we can also rewrite it into a first order system:

$$q_t + 4s - p_x = 0,$$

$$p - s_x = 0,$$

$$s - f(u)_x = 0.$$

The LDG method (I) continued

Find $q_h, p_h, s_h \in V_h$ such that, $\forall \varphi, \psi, \eta \in V_h$,

$$\int_{I_j} (q_h)_t \varphi dx + \int_{I_j} 4s_h \varphi dx + \int_{I_j} p_h \varphi_x dx - (\widehat{p}_h \varphi^-)_{j+\frac{1}{2}} + (\widehat{p}_h \varphi^+)_{j-\frac{1}{2}} = 0,$$

$$\int_{I_j} p_h \psi dx + \int_{I_j} s_h \psi_x dx - (\widehat{s}_h \psi^-)_{j+\frac{1}{2}} + (\widehat{s}_h \psi^+)_{j-\frac{1}{2}} = 0,$$

$$\int_{I_j} s_h \eta dx + \int_{I_j} f(u_h) \eta_x dx - (\widehat{f} \eta^-)_{j+\frac{1}{2}} + (\widehat{f} \eta^+)_{j-\frac{1}{2}} = 0.$$

The numerical fluxes are chosen as

$$\widehat{p}_h = p_h^-, \quad \widehat{s}_h = s_h^+,$$

and $\widehat{f}(u_h^-, u_h^+)$ is a central flux or Lax-Friedrichs flux.

Algorithm flowchart (I)

- We obtain q_h in the following matrix form

$$\mathbf{q}_h = \mathbf{A}u_h.$$

- we obtain the LDG discretization of the residual $4f(u)_x - f(u)_{xxx}$ in the vector form

$$(\mathbf{q}_h)_t = \mathbf{res}(u_h).$$

- We then combine the above two equation to obtain

$$\mathbf{A}(u_h)_t = \mathbf{res}(u_h).$$

- We use a time discretization method to solve

$$(u_h)_t = \mathbf{A}^{-1}\mathbf{res}(u_h).$$

LDG scheme (II) based on hyperbolic-elliptic form

We write the DP equation in the following form

$$\begin{aligned}u_t + f(u)_x + p &= 0, \\ p - p_{xx} &= 3f(u)_x.\end{aligned}$$

We rewrite the equation as a first order system:

$$\begin{aligned}u_t + q + p &= 0, \\ p - s_x &= 3q, \\ s - p_x &= 0, \\ q - f(u)_x &= 0.\end{aligned}$$

LDG scheme (II) continued

Find $u_h, s_h, p_h, q_h \in V_h$ such that, $\forall \varphi, \psi, \eta \in V_h$,

$$\int_{I_j} (u_h)_t \varphi dx + \int_{I_j} (q_h + p_h) \varphi dx = 0,$$

$$\int_{I_j} p_h \psi dx + \int_{I_j} s_h \psi_x dx - (\widehat{s}_h \psi^-)_{j+\frac{1}{2}} + (\widehat{s}_h \psi^+)_{j-\frac{1}{2}} = 3 \int_{I_j} q_h \psi dx,$$

$$\int_{I_j} s_h \eta dx + \int_{I_j} p_h \eta_x dx - (\widehat{p}_h \eta^-)_{j+\frac{1}{2}} + (\widehat{p}_h \eta^+)_{j-\frac{1}{2}} = 0,$$

$$\int_{I_j} q_h \rho dx + \int_{I_j} f(u_h) \rho_x dx - (\widehat{f} \rho^-)_{j+\frac{1}{2}} + (\widehat{f} \rho^+)_{j-\frac{1}{2}} = 0.$$

Numerical fluxes are chosen as

$$\widehat{p}_h = p_h^-, \widehat{s}_h = s_h^+.$$

Here $\widehat{f}(u_h^-, u_h^+)$ is a central flux or Lax-Friedrichs flux.

Algorithm flowchart (II)

- Given the solution u_h at time level n , we first get \mathbf{q}_h .

$$\mathbf{q}_h = \mathbf{res}(\mathbf{u}_h).$$

- We obtain p_h in the following matrix form

$$\mathbf{p}_h = 3\mathbf{A}^{-1}\mathbf{q}_h.$$

- Using the solution $\mathbf{q}_h, \mathbf{p}_h$ to computing discretization of the residual $p + q$, then we obtain

$$(\mathbf{u}_h)_t = \mathbf{q}_h + \mathbf{p}_h.$$

Any standard ODE solvers can be used here, for example the Runge-Kutta methods.

Stability of the LDG method (I) and (II)

- Energy stability of the solution v_h
 - $\hat{f}(u_h^-, u_h^+)$: central numerical flux

$$\frac{d}{dt} \int_{\Omega} \left(2v_h^2 + \frac{5}{2}w_h^2 + \frac{1}{2}z_h^2 \right) dx = 0.$$

- $\hat{f}(u_h^-, u_h^+)$: Lax-Friedrichs flux

$$\frac{d}{dt} \int_{\Omega} \left(2v_h^2 + \frac{5}{2}w_h^2 + \frac{1}{2}z_h^2 \right) dx \leq 0.$$

where w_h and z_h are approximation of v_x and v_{xx} .

- L^2 stability of solution u_h

$$\|u_h\|_{L^2(\Omega)} \leq 2\sqrt{2}\|u_0\|_{L^2(\Omega)}.$$

Total variation bounded property for the P^0 case

$$\text{TVM}(u_h^n) \leq \exp(CT)\text{TVM}(u^0),$$

where $\text{TVM}(u_h) = \sum_{j=1}^J |\Delta_+ u_j|$.

Outline

- 1 Introduction to local discontinuous Galerkin (LDG) methods
- 2 The LDG method for the Camassa-Holm equation
- 3 LDG method for the Degasperis-Procesi equation
- 4 Numerical results
 - Numerical results for the CH equation
 - Numerical results for Degasperis-Procesi equation
- 5 Conclusion and future work

Smooth solution

Smooth traveling waves are solution of the form

$$u(x, t) = \phi(x - ct)$$

where ϕ is solution of second-order ordinary differential equation

$$\phi_{xx} = \phi - \frac{\alpha}{(\phi - c)^2}.$$

$\alpha = c = 3$. The initial conditions for ϕ is

$$\phi(0) = 1, \quad \frac{d\phi}{dx}(0) = 0.$$

It gives rise to a smooth traveling wave with period
 $a \simeq 6.46954603635$.

Table: Accuracy test for the CH equation. Periodic boundary condition. Uniform meshes with N cells at time $t = 0.5$.

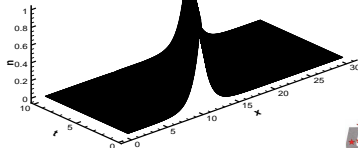
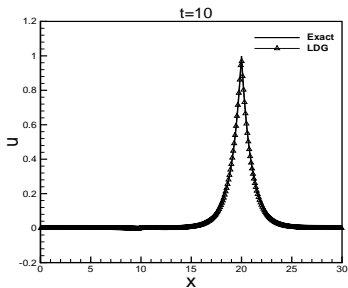
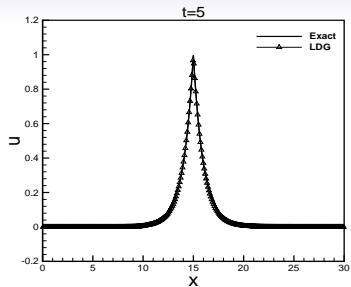
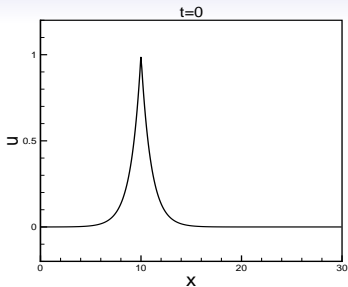
	N	$u - u_h$				$r - r_h$			
		L^2 error	order	L^∞ error	order	L^2 error	order	L^∞ error	order
P^0	10	1.42E-01	–	3.08E-01	–	1.42E-01	–	3.08E-01	–
	20	7.95E-02	0.84	1.77E-01	0.80	7.95E-02	0.83	1.77E-01	0.57
	40	4.23E-02	0.91	9.41E-01	0.91	4.23E-02	0.94	9.41E-02	0.87
	80	2.18E-02	0.95	4.83E-02	0.96	2.18E-02	0.98	4.83E-02	0.97
P^1	10	1.16E-02	–	6.63E-02	–	1.16E-02	–	6.63E-02	–
	20	3.12E-03	1.90	1.86E-02	1.84	3.12E-03	0.68	1.86E-02	0.24
	40	8.05E-04	1.95	4.76E-03	1.96	8.05E-04	0.85	4.76E-03	0.63
	80	2.04E-04	1.98	1.19E-02	2.00	2.04E-04	0.93	1.19E-03	0.87
P^2	10	1.41E-03	–	6.75E-03	–	1.41E-03	–	6.75E-03	–
	20	1.49E-04	3.24	9.06E-04	2.90	1.49E-04	2.64	9.06E-04	2.64
	40	1.70E-05	3.13	9.85E-05	3.20	1.70E-05	2.06	9.85E-05	1.45
	50	8.95E-06	2.88	4.96E-05	3.07	8.95E-06	1.95	4.96E-05	1.77

Peakon solution

In the single peak case, the initial condition is

$$u_0(x) = \begin{cases} \frac{c}{\cosh(a/2)} \cosh(x - x_0), & |x - x_0| \leq a/2, \\ \frac{c}{\cosh(a/2)} \cosh(a - (x - x_0)), & |x - x_0| > a/2, \end{cases}$$

where x_0 is the position of the trough and a is the period. We present the wave propagation for the CH equation with parameters $c = 1$, $a = 30$ and $x_0 = -5$. The computational domain is $[0, a]$. P^5 element with $N = 320$ cells.



Two-peakon interaction

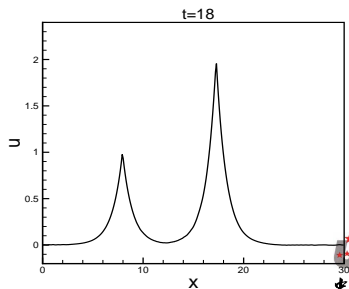
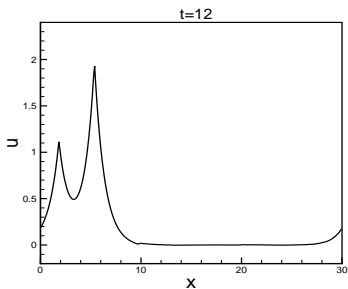
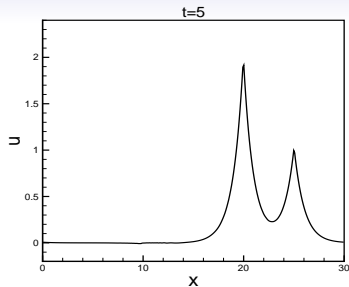
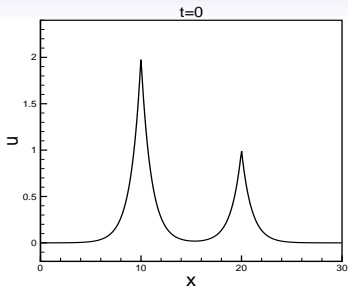
In this example we consider the two-Peakon interaction of the CH equation with the initial condition

$$u_0(x) = \phi_1(x) + \phi_2(x),$$

where

$$\phi_i(x) = \begin{cases} \frac{c_i}{\cosh(a/2)} \cosh(x - x_i), & |x - x_i| \leq a/2, \\ \frac{c_i}{\cosh(a/2)} \cosh(a - (x - x_i)), & |x - x_i| > a/2, \end{cases} \quad i = 1, 2.$$

The parameters are $c_1 = 2$, $c_2 = 1$, $x_1 = -5$, $x_2 = 5$, $a = 30$. The computational domain is $[0, a]$. P^5 element with $N = 320$ cells.

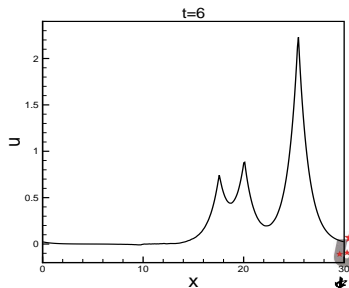
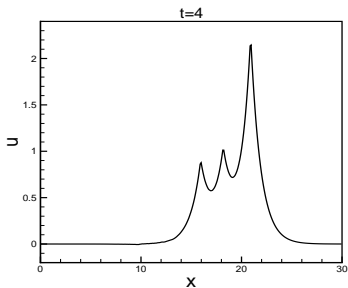
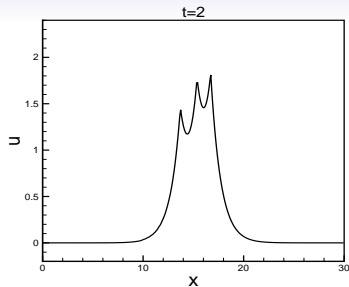
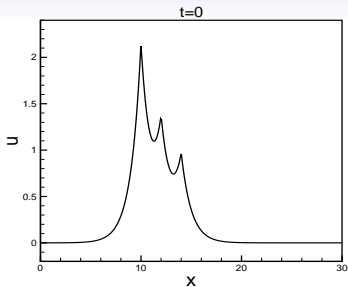


Three-peakon interaction

In this example we consider the three-Peakon interaction of the CH equation with the initial condition

$$u_0(x) = \phi_1(x) + \phi_2(x) + \phi_3(x),$$

where ϕ_i , $i = 1, 2, 3$ are defined as before. The parameters are $c_1 = 2$, $c_2 = 1$, $c_3 = 0.8$, $x_1 = -5$, $x_2 = -3$, $x_3 = -1$, $a = 30$. The computational domain is $[0, a]$. P^5 element with $N = 320$ cells.

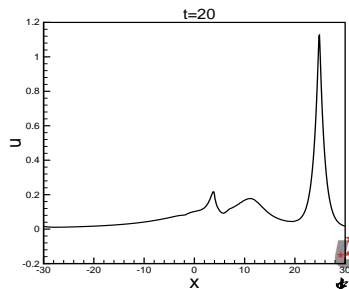
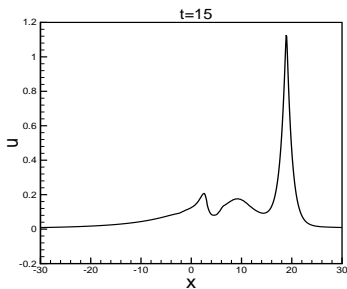
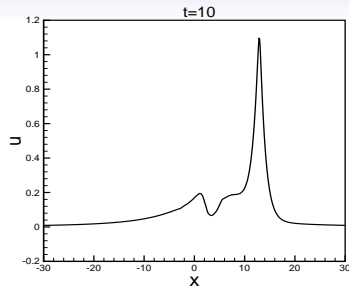
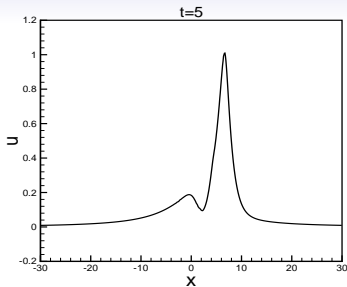


Solution with a discontinuous derivative

In this example we consider a initial data function u_0 which has a discontinuous derivative. The initial condition is

$$u_0(x) = \frac{10}{(3 + |x|)^2}.$$

The computational domain is $[-30, 30]$. P^2 element with $N = 640$.

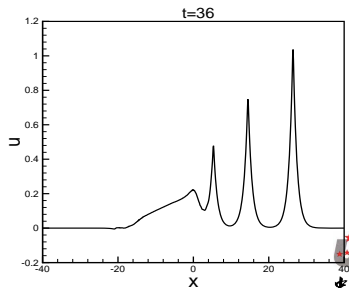
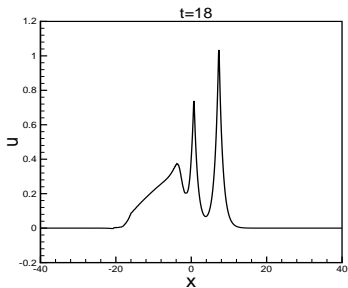
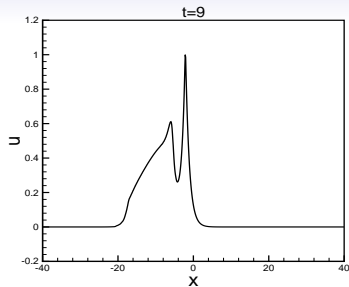
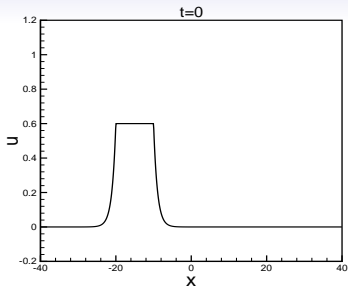


Break up of the plateau traveling wave

A cut-off peakon, i.e. a plateau function $u(x, t) = \phi(x - ct)$ with

$$\phi(x) = \begin{cases} ce^{x+k}, & x \leq -k, \\ c, & |x| \leq k, \\ ce^{-x+k}, & x \geq k. \end{cases}$$

We put $c = 0.6$ and $k = 5$. The computational domain is $[-40, 40]$. P^2 element with $N = 800$ cells.



Outline

- 1 Introduction to local discontinuous Galerkin (LDG) methods
- 2 The LDG method for the Camassa-Holm equation
- 3 LDG method for the Degasperis-Procesi equation
- 4 Numerical results**
 - Numerical results for the CH equation
 - Numerical results for Degasperis-Procesi equation
- 5 Conclusion and future work

Accuracy test

Table: Accuracy test for the DP equation with the exact solution $u(x, t) = ce^{-|x-ct|}$. Periodic boundary condition. $c = 0.25$. Uniform meshes with N cells at time $t = 1$.

	N	Scheme (I)				Scheme (II)			
		L^2 error	order	L^∞ error	order	L^2 error	order	L^∞ error	order
p^0	20	6.62E-03	–	6.84E-02	–	6.62E-03	–	6.84E-02	–
	40	1.98E-03	1.74	2.18E-02	1.65	1.98E-03	1.74	2.18E-02	1.65
	80	8.56E-04	1.21	1.02E-02	1.09	8.56E-04	1.21	1.02E-02	1.09
	160	4.76E-04	0.85	6.39E-03	0.68	4.76E-04	0.85	6.39E-03	0.68
p^1	20	2.31E-03	–	3.19E-02	–	2.31E-03	–	3.19E-02	–
	40	1.73E-04	3.74	2.42E-03	3.71	1.73E-04	3.74	2.43E-03	3.71
	80	3.92E-05	2.14	5.31E-04	2.19	3.92E-05	2.14	5.31E-04	2.19
	160	1.08E-05	1.86	1.88E-04	1.50	1.08E-05	1.86	1.88E-04	1.50
p^2	20	3.90E-04	–	6.61E-03	–	3.90E-04	–	6.61E-03	–
	40	3.35E-05	3.54	5.25E-04	3.93	3.35E-05	3.54	4.33E-04	3.93
	80	4.07E-06	3.04	5.25E-05	3.04	4.07E-06	3.04	5.25E-05	3.04
	160	5.77E-07	2.82	7.13E-06	2.88	5.77E-07	2.82	7.13E-06	2.88
p^3	10	1.49E-03	–	1.77E-02	–	1.49E-03	–	1.77E-02	–
	20	1.51E-04	3.30	2.69E-03	2.72	1.51E-04	3.30	2.69E-03	2.72
	40	7.64E-06	4.30	1.32E-04	4.35	7.64E-06	4.31	1.32E-04	4.36
	80	1.60E-07	5.58	2.13E-06	5.95	1.60E-07	5.58	2.13E-06	5.95
p^4	10	7.07E-03	–	7.09E-02	–	7.07E-03	–	7.09E-02	–
	20	1.72E-04	5.36	2.75E-03	4.69	1.72E-04	5.36	2.76E-03	4.68
	40	4.68E-06	5.20	8.45E-05	5.02	4.68E-06	5.20	8.45E-05	5.03
	80	8.30E-08	5.82	1.31E-06	6.01	8.30E-08	5.82	1.31E-06	6.01

Peakon solution

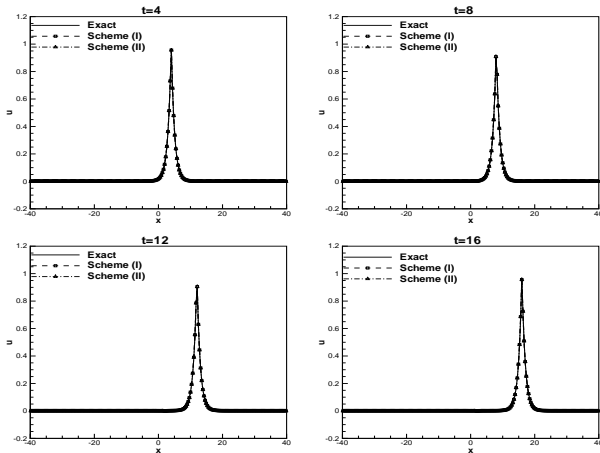


Figure: The peakon profile of the DP equation with the exact solution $u(x, t) = e^{-|x-t|}$. Periodic boundary condition in $[-40, 40]$. P^4 elements and a uniform mesh with $N = 228$ cells.

Two-peakon interaction

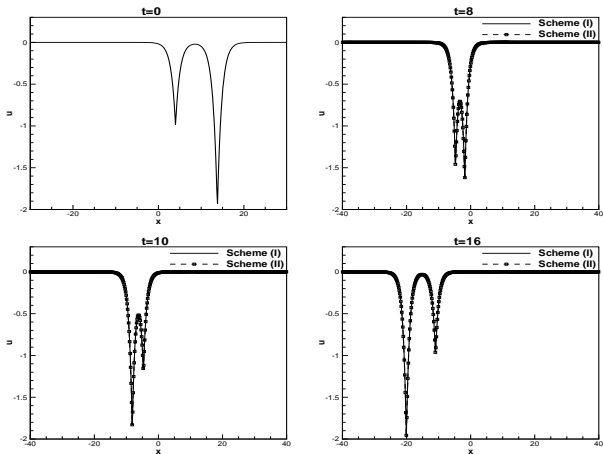


Figure: The two-anti-peakon interaction of the DP equation. Periodic boundary condition in $[-40, 40]$. P^3 elements and a uniform mesh with $N = 512$ cells.

Shock peakon solution

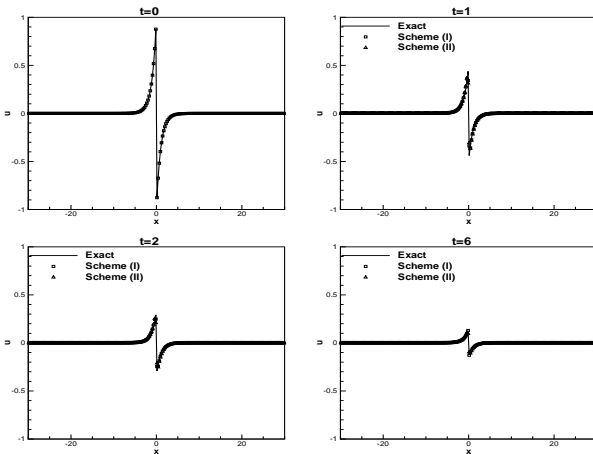


Figure: Shock peakon solution of the DP equation with the exact solution $u(x, t) = -\text{sign}(x)e^{-|x|}/(1+t)$. Periodic boundary condition in $[-30, 30]$. P^4 elements and a uniform mesh with $N = 228$ cells.

Shock formation

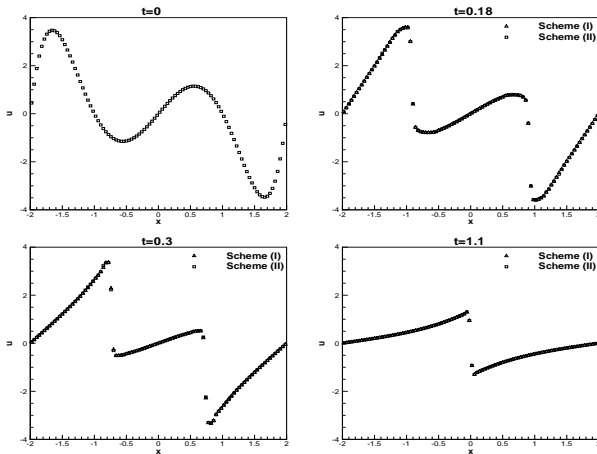


Figure: Shock formation of the DP equation with the initial condition $u_0(x) = e^{0.5x^2} \sin(\pi x)$. Periodic boundary condition in $[-2, 2]$. P^3 elements and a uniform mesh with $N = 100$ cells.

Peakon and anti-Peakon interaction (Symmetric)

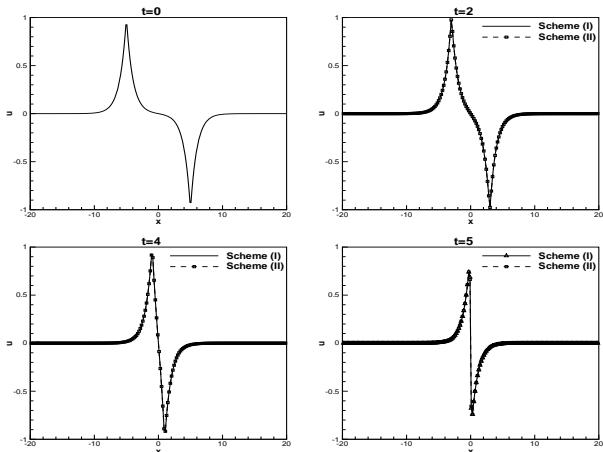


Figure: Symmetric peakon and antipeakon interaction of the DP equation. Periodic boundary condition in $[-25, 25]$. P^3 elements and a uniform mesh with $N = 256$ cells.

Peakon and anti-Peakon interaction (Nonsymmetric)

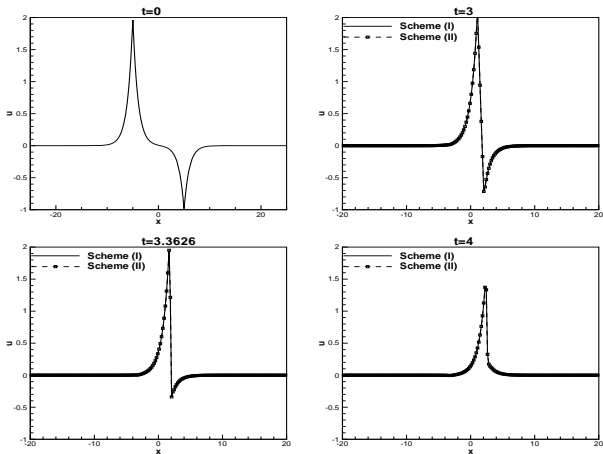


Figure: Nonsymmetric peak and antipeak interaction of the DP equation. Periodic boundary condition in $[-25, 25]$. P^3 elements and a uniform mesh with $N = 256$ cells.

Triple interaction

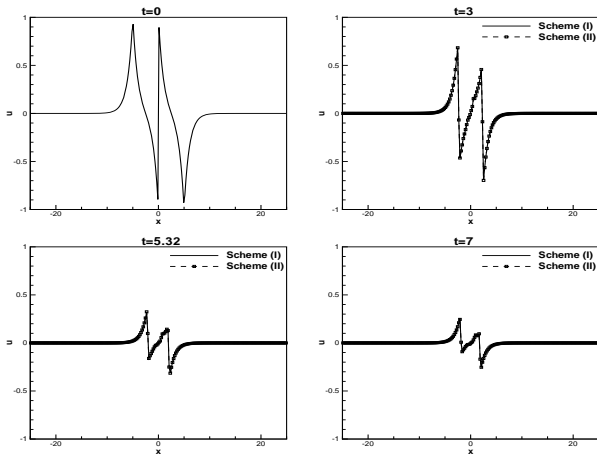


Figure: Peakon, shock peakon and anti-peakon of the DP equation. Periodic boundary condition in $[-25, 25]$. P^3 elements and a uniform mesh with $N = 256$ cells.

- ① Introduction to local discontinuous Galerkin (LDG) methods
- ② The LDG method for the Camassa-Holm equation
- ③ LDG method for the Degasperis-Procesi equation
- ④ Numerical results
 - Numerical results for the CH equation
 - Numerical results for Degasperis-Procesi equation
- ⑤ Conclusion and future work

Conclusion

- LDG methods to solve the nonlinear equation.
- Stability is proven for the schemes for general solutions .
- Numerical examples are given to illustrate the accuracy and capability of the methods.

Future work

- Total variation bounded property for the high order case.
- a priori error estimates of numerical solutions.

Reference

More information about the algorithm and theoretical analysis can be found in:

<http://staff.ustc.edu.cn/~yxu/>